Al-Nahrain Journal of Science
ANJS, Vol.27(3), September, 2024, pp. 69-80

Comparison of the Effectiveness of 532 nm and 660 nm Diode Laser on MRSA Viability in Different Tissue Thicknesses in Vitro

Ali A. Turki Aldalawi*

Department of Vocational Education, Babylon Education Directorate, Babylon, Iraq

Article's Information

Received: 02.04.2024
Accepted: 05.06.2024
Published: 15.09.2024

Keywords:
Diode laser
Tissue thickness
MRSA infection
Treatment effectiveness
Bacterial viability

Abstract

Laser-based technologies are indispensable tools in microbial decontamination and provide effective means for controlling infectious agents across diverse environments. However, understanding the transmission of laser light through different tissue types is crucial for optimizing microbial control efficacy and patient safety. This study investigates the interaction between laser parameters and tissue properties, focusing on the effect of 532 nm and 660 nm diode lasers on Methicillin-resistant Staphylococcus aureus MRSA susceptibility in chicken and beef tissues with different thicknesses. By investigating the interplay between laser parameters and different tissue properties, including penetration depth and transmission properties, this study provides valuable insights for improving laser-based microbial decontamination strategies. These insights facilitate the development of personalized treatment protocols that take into account tissue-specific optical properties, ensuring precise targeting of microbial pathogens while minimizing potential damage to surrounding tissue. Wavelengths of 660 nm significantly reduced MRSA viability in 3 mm thick beef samples, promising tissue safety. Conversely, 532 nm wavelengths were most effective in 5 mm and 10 mm thick beef samples, demonstrating laser-based versatility in targeting microbial pathogens across tissue environments. By elucidating optimal laser parameters for diverse tissues, this research lays the foundation for personalized treatment protocols against MRSA in various clinical settings. These results provide valuable insights into understanding the interaction between laser light and tissue properties and mitigating potential risks associated with laser-based interventions. As such, incorporating considerations of penetration depth and transmission characteristics into laser treatment planning is essential to achieve optimal microbial control outcomes and ensure patient safety across diverse tissue environments.

http://doi.org/10.22401/ANJS.27.3.09
*Corresponding Author Email: alialdalawi87@gmail.com

1. Introduction

Laser technology is now considered one of the most effective disinfection methods as it provides a very high level of accuracy and thoroughness [1,2]. Among the broad parameters of lasers used in addressing this issue, the eradication of Methicillin-resistant Staphylococcus aureus (MRSA) is a major objective that cannot be achieved with conventional antibiotic treatments due to the MRSA's resistance to it [3]. In particular, the wavelengths at 532 nm and 660 nm are characterized by their photochemical and photothermal impacts on bacterial cells [4,5]. Although there is increasing interest in these applications, healthcare providers know little about diode lasers response to tissue thickness variation [6]. Although the introduction of lasers as a mechanism for microbial decontamination shows an overall increase in its adoption, there is still a need to understand the specific effects that different wavelengths bring on MRSA within tissues of different thicknesses [7]. Selecting the appropriate laser wavelength is imperative because it decides the

degree of photochemical and photothermal effects in the biological tissues [8]. Furthermore, tissue thickness is a significant parameter, which affects the efficiency of diode-laser-based interventions [9]. This study focuses on highlighting these gaps by comparing the impact of diode lasers with wavelengths 532nm and 660nm on the MRSA contamination level. The investigation of different tissue thicknesses, ranging from 3 mm to 10 mm, is the aim of this study to offer insight into MRSA action specific to wavelengths in different biological environments. Besides contributing to the basic principles of laser-microbe interactions, the results of this research will also be useful for developing optimal strategies to control microbes in different types of tissues, which will change clinical practice and enhance public health prospects.

2. Materials and Methods

i. Tissue Collection

Chicken breast and beef tissues were obtained from reputable local suppliers to prepare the experimental samples, following ethical guidelines and standards. The procedure included checking for any visible defects, malformations, or indications of damage. To simulate different biological tissue environments, chicken and beef breast tissues were carefully divided into three thickness classes using vernier calipers and a scalpel: 3 mm, 5 mm, and 10 mm, as an index of maximum light penetration estimated on different tissue, including (1, 3, 5,10, 20) mm (Figure 1). The selection of these thicknesses ensures coverage of a range of penetration depths relevant to antimicrobial treatment. For example, shorter wavelengths can penetrate less deeply, while longer wavelengths can penetrate deeper into tissue [1]. However, this difference enhances the study's statistical power and provides a more comprehensive understanding of how tissue characteristics influence treatment results [2]. Thickness standardization within each category was carefully monitored to avoid confusing factors that might bias the results. Careful handling of tissue samples has been given preference so as not to cause any damage or contamination. Sterile instruments were used for sectioning, and all procedures were performed in a laboratory environment free of external influences. The tissues were collected and conserved in an appropriate environment immediately after sampling. To prevent microbial colonization growth or the degradation of tissue quality, a refrigeration temperature of 4°C was used. Tissue samples were individually packaged to ensure no cross-contamination, and were stored in sealed tubes. Periodic monitoring was performed by randomly selecting samples to estimate the quality and integrity of the tissues during the trial period. Samples that deteriorated or tended to reduce the data quality were immediately replaced to ensure the accuracy of the experimental results. Storage, management, and keeping of these procedures ensure tissue integrity, making experimental results accurate and reproducible.

Figure 1. Tissue preparation into slices of different thicknesses

ii. Microbial Strain

In this study, MRSA strains of methicillin-resistant Staphylococcus aureus were selected with extreme caution as the experimental microbial contaminants. The investigation of MRSA as one of the main antibiotic-resistant bacteria is one of the more interesting challenges in the microbial decontamination area [10]. The approved bacterial strain designated with antibiotic resistance can serve as a model for the efficacy of diode lasers in treating microbial contamination. A culture of MRSA was accomplished in a sterile environment and with the appropriate growth media at 37 °C for 24 hours before the experiment. The culture conditions were selected to support the metabolic pathways of MRSA and promote their growth and viability [11]. By measuring the optical density the concentration of the bacterial suspension was estimated as 5 McFarland (1.5×109 CFU), obtaining a standardized concentration [12]. The same result was also shown while performing other microbiological analyses. Sample backs from various localities on each tissue sample enabled the verification of homogenous MRSA spread across the specimen [12]. This method was able to fulfill dual objectives including being a perfect representation of real situations and providing an atmosphere for the accurate evaluation

of the outcome of diode lasers on MRSA at different tissue thicknesses.

iii. Experimental Groups

The experiment included two control groups that were conducted to examine baselines and MRSA survival rates without laser treatment, as follows:

iv. Blank (unstained) tissue sample group

The unstained tissue samples were the reference values and were used to determine the starting measurements. While keeping the sample free of any intentional spreading of MRSA infections. The function behind the application of this control group was to provide a point for comparison of intrinsic tissue features devoid of the external context of the microorganisms. The samples received the same processing, storage, and testing protocols as with the control and the experiment group, but without being intentionally contaminated or exposed to the laser treatment.

v. Contaminated tissue samples without laser treatment (viability control)

MRSA-contaminated tissue samples, that were not treated, were included to determine the natural survival of MRSA under experimental conditions. This control group made it possible to compare the survival of MRSA without diode laser interaction. It served as a reference for the effectiveness of diode laser treatment in terms of bacterial viability. Placing control groups was appropriate to figure out the basic traits of non-infected tissues and measure MRSA's base viability without any laser intervention [13]. By contrasting the data of the control groups with the data of the experimental groups, the effects of the diode laser on the survival of MRSA within different tissue layers were determined. All control groups were randomly distributed within the experimental design to avoid bias. To improve the reliability and validity of the control group data, each control group was replicated (n=3). These control groups were of great importance for interpreting the effect of the laser on MRSA within different tissue environments, as they acted as a consistent standard for understanding the experiment results.

vi. The laser-treated group and the viability analysis

The study protocol was an experiment in which samples were intentionally contaminated with MRSA, and then after control irradiated with a diode laser at two different wavelengths, 532 nm, and 660 nm, at specific energy densities of 167 J/cm² for 532 nm and 142 J /cm² for 660 nm. When considering the use of two different laser wavelengths, it is important to note the individual tissue penetration characteristics of each wavelength. This study makes it easier for medical professionals to evaluate how differences in wavelength affect the depth of penetration, thus this assessment in turn affects antimicrobial efficacy against MRSA viability across different tissue thicknesses [14,15]. In addition, the study controlled various factors such as energy settings, exposure time, and thermal effect on tissue during laser irradiation by setting the energy density to 167 J/cm² for 532 nm and 142 J/cm² for 660 nm. Understanding and managing these thermal effects is essential to ensure the safety and effectiveness of antimicrobial therapies in clinical settings [3]. This approach is of primary importance for promoting and developing laser-based technologies in the field of microbial control. To test MRSA viability after laser treatment, the McFarland turbidity was measured for the maximum concentration (1.5×10^9 CFU) [14,15]. The results of MRSA viability were diligently documented for the experimental and control groups using the quantitative data approach. By applying the CFU/ml technique, numerical data were obtained, which informs a quantitative measure of the viability of MRSA colonies and can therefore be qualitatively interpreted as bacterial survival. Careful and stringent procedures were in place to ensure valid and informative data collection with no variability during CFU/ml counting procedures, which followed standard protocols in all the samples. This methodology was fundamental to ensuring correctness and dependability in assessing MRSA viability under laser radiation. Therefore, each experimental group for both wavelengths was divided into three subgroups (n = 3) based on tissue thickness. These subgroups underwent vertical laser irradiation in continuous mode for 10 minutes under dark conditions, followed by comparison with control groups. This treatment duration was included to optimize antimicrobial efficacy while mitigating potential tissue damage due to excessive heating, as reported in several publications. Longer exposure may enhance bacterial killing but pose a greater risk of tissue damage, while shorter periods may affect microbial reduction. Continuous mode also ensures consistent delivery of laser energy, aiding in sustained thermal effects and uniform treatment across the thickness of the tissue. In addition, it simplifies experimental procedures and data analysis and enhances reproducibility. Subdivision allows for

a detailed examination of how tissue thickness affects laser treatment response, aiding in understanding the effects of laser on antimicrobial efficacy across different tissue depths.

vii. Experimental design

Before undergoing irradiation, 36 tissue samples were classified into three distinct test groups: the blank, control, and irradiated groups, each comprising three samples (n = 3), as shown in Figure 2. The tissue samples, consisting of a control and a treatment group, were placed into an aluminum box specially made for irradiation. The box was designed to include, with great precision, a wooden platform that was installed together with proper barriers to control the scattering or reflection of the laser. So far it has been proven that the scattering and reflection of laser light can break down the energy concentrated in one point which can decrease the treatment effect if the energy is spread to a larger area and thus, the intensity of the light is reduced [14,16]. To ensure the maximum transmission of the laser light in different tissues, the power meter recorded the intensity of the light transmitted through the tissue for various tissue thicknesses, namely 1, 3, 5, 10, and 20 mm before any staining or treatment begins. This process was performed to detect the efficiency of light transmission through the tissue which is a primary factor in determining treatment efficiency and preventing inconsistent results across different tissue thicknesses [17,18]. The measurement process is represented by the Equation:

$$T = \frac{I}{I_o} \times 100\ \% \qquad \ldots (1)$$

where T is the light transmission, I represents transmission intensity (W/cm^2) at the tissue surface, and I_0 Indicates the intensity of the incident light transmitted through the tissue samples, as shown in the results section. The scattering or reflection of these waves may hinder their transmission to such depth that microbes will not receive sufficient lethal doses, potentially allowing them to find refuge in deeper layers of the skin [19]. To mitigate this problem, the laser device was directed vertically into the center of each sample to achieve a uniform sample-spot distance of 1 to 2 cm, as shown in Figure 3. This positioning enhanced the efficiency of the treatment and decreased any problems that may arise from the laser's penetration or scattering into different mediums [4]. This approach improves treatment effectiveness by ensuring consistent and focused laser energy delivery while reducing the potential for scattering or energy loss caused by reflection [5].

Before irradiation, each sample underwent inoculation with MRSA. A microbial suspension, consisting of 30 µl at a concentration of 5 McFarland (1.5×10^9 CFU), was pipetted onto the surfaces of the tissue samples. These inoculated samples were then allowed to incubate for 30 minutes, facilitating the effective penetration of bacteria into the tissue surfaces. This incubation period provides sufficient time for MRSA bacteria to adhere to the tissue surface, which matches the normal state in which bacteria can colonize biological tissues prior to treatment. Using uniform treatment duration and achieving the desired treatment results across all samples, an exposure time of 10 minutes was set. A comparative analysis was then performed by creating several decimal dilutions to compare with the zero dilution [6]. A smear layer of 150 µl was blotted onto mannitol salt agar to achieve a 0.5 McFarland standard concentration [20,21]. The samples were then incubated at 37°C for 24 hours to enumerate the microorganisms growing on the agar layer, which represented the CFU/ml remaining after laser irradiation for the control, experimental, and blank groups under tightly controlled laboratory conditions.

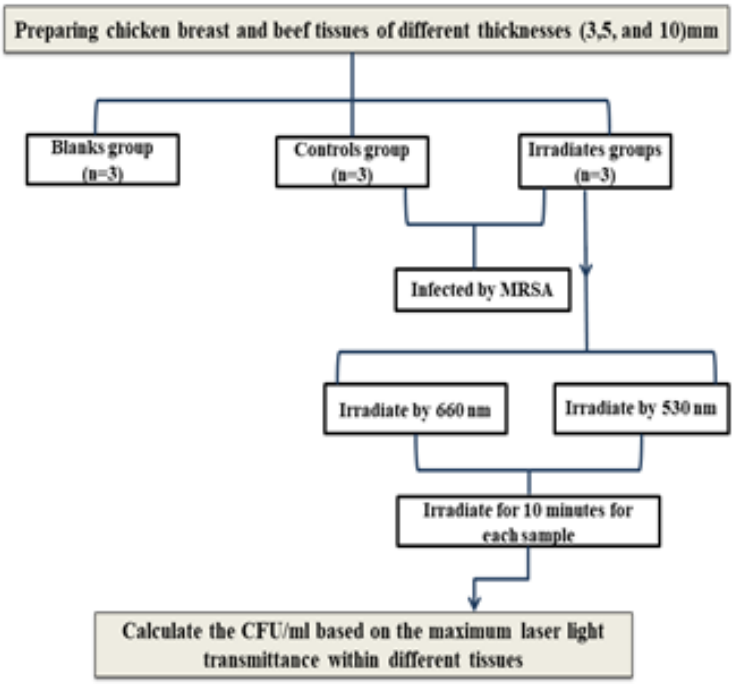

Figure 2. Experimental work processes.

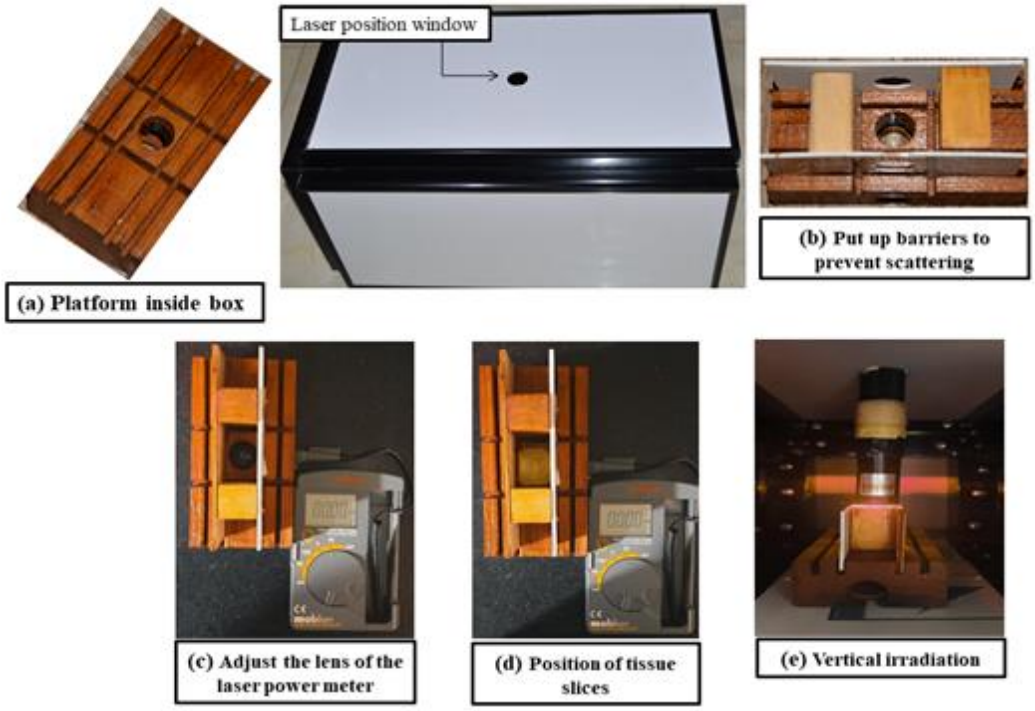

Figure 3. Preparation of the experimental setup involves the following components: (a) Arranging a movable wooden platform within the box to accommodate the samples (b) Establishing the placement of barriers around the samples (c) Installing the lens for the laser power meter (d) Identifying the specific location for the tissue samples (e) Implementing a vertical irradiation mechanism.

viii. Statistical Analysis

Two-way ANOVA was performed to evaluate potential interaction effects between laser wavelength and tissue thickness on MRSA viability. The results of all tests were compared and presented as mean ± SD. This analysis aimed to determine whether the combined effect of different wavelengths and tissue thickness resulted in synergistic or antagonistic effects on bacterial survival. The significance of differences for each treatment was determined by calculating the p-value. A p-value less than 0.05 was deemed statistically significant, while a p-value exceeding 0.05 was considered not statistically significant.

3. Results and Discussion

3.1. Light Transmission Measurement

Analysis of the results revealed differences in light transmission efficiency across different tissue thicknesses, as shown in Table 1 and Figure 4 for beef tissue, along with Table 2 and Figure 5 for chicken breast tissue, this can be attributed to various factors related to composition, shape, and optical properties. In the case of beef tissue, the mean measured transmission spectra across different thicknesses reveal significant differences in optical transmissions at wavelengths of 660 nm and 532 nm. These variations are particularly notable from the initial moment of laser irradiation up to the end of 10 minutes, indicating that the tissue composition and structure influence how laser beams penetrate and interact with the tissue. Similarly, the comparison of mean transmission light for various thicknesses of chicken breast and beef tissue also highlights significant disparities between initial and final permeations, emphasizing the impact of tissue thickness on laser penetration. Overall, the observed differences in light transmission efficiency across different tissue thicknesses underscore the importance of considering tissue properties when designing laser-based therapies. Understanding these differences is critical to improving treatment outcomes and ensuring antimicrobial efficacy against pathogens such as MRSA.

3.2. MRSA Viability Count

A significant decrease ($P < 0.05$) in the MRSA viability index was revealed in all treatment groups of beef tissues compared to the control group. The mean p-values for 532 nm and 660 nm laser-treated groups were 0.003 and 0.002, respectively. This is in contrast to the average p-values for all control groups of 0.146 and 0.190 for the 532 nm and 660 nm exposure, respectively. In particular, a more significant reduction in MRSA viability was observed in 3 mm tissue (P value: 0.003) when treated with the 532 nm laser, compared to 5 mm and 10 mm. In addition, a greater reduction in MRSA viability was observed in 3 mm thickness tissues (P value: 0.001) when exposed to 660 nm, compared to those with 5 mm and 10 mm thickness. These results are shown in Table 3 and Figure 6. On the other hand, a significant decrease ($P < 0.05$) in the MRSA viability index was noted in all treatment groups of chicken breast tissues over the control group. Mean p-values for the 532 nm laser and 660 nm laser treated groups were 0.001 and 0.002, respectively, compared with mean p-values of 0.626 and 0.136 for the 532 nm and 660 nm wavelengths, respectively for all control groups. In particular, a greater reduction in MRSA viability was observed in 3 mm tissue (P value: 0.001) when treated with the 532 nm laser, compared to 5 mm and 10 mm. On the other hand, a significant reduction in MRSA viability was observed in 10 mm thick tissues (P value: 0.006) when treated with 660 nm laser, compared to those with 5 mm thickness and 3 mm thickness. These results are documented in Table 4 and Figure 7.

4. Discussion

The diverse viabilities of MRSA in 532 nm and 660 nm wavelengths revealed the wavelength-specific impacts of the diode laser on the pathogen. This evidence fits in with previous studies which showed that different wavelengths have specific photochemical and photothermal effects on bacterial cells [22], [23]. The 532 nm wavelength which is located in the green visible spectrum and the 660 nm wavelength which is located in the red spectrum, interact differently with MRSA cells. As a result, it affects their survival rates. However, the pronounced MRSA survival in the presence of different tissue depths calls for thoroughness in the tissue properties of laser-based microbial killing [24]. Literature evidence has shown thicker tissue reduces the depth of light penetration and its absorption [25]. The results suggest that laser effectiveness is not only related to wavelength, but the layer of the target tissue can also affect the treatment [26]. This information will help determine the use of laser in situations where microbial contaminants are present at different levels of tissues [7]. It has been realized that the type of wavelength used was of great importance to the light depth that could penetrate the tissue. Firstly, the specific long wavelength of 660 nm has the deepest penetration compared to the

short wavelength of 532 nm. However, this is a very crucial factor determining the path of laser energy through tissue, therefore, affecting the survivability of MRSA. The absorption and scattering of biological tissues are multi-layered with different wavelengths on both sides of the parallelism [26], which leads to distinct ways the MRSA interacts with the lasers and subsequently influences the detected changes in viability. The study further uncovers that distinct wavelengths can evoke unique photobiological responses in biological systems. The mechanisms through which the 660 nm and 532 nm wavelengths interact with MRSA differ, involving bacterial cell penetration and subsequent cellular damage, leading to distinct effects on viability [27]. Cellular and molecular responses of MRSA to light exposure display variability based on wavelength, with cellular structures and targets within MRSA responding distinctly to the energy provided by 660 nm and 532 nm lasers. However, the results of the current study are consistent with existing literature on microbial decontamination using lasers, providing additional evidence of wavelength and tissue thickness dependencies [28]. Comparisons with studies investigating similar parameters revealed light transmission and penetration depth as critical factors for direct assessment of the effect on microbial cells within tissue boundaries [29,30], providing insight into microbial membrane damage and healing mechanisms, further supporting the generalizability of the in vivo findings. Based on these results, future research can explore the effect of additional laser parameters, such as pulse duration and energy density, on MRSA viability. In addition, evaluating the applicability of these findings in more complex biological settings or in vivo models would contribute to a more comprehensive understanding. However, incorporating diode laser impact on MRSA viability in clinical trials can give an account of in vivo results and consequently assist in translation into viable clinical applications. In vivo models offer a more complete and detailed perspective of the biocontrol phenomenon where many factors interact in the real host environment.

Table 1. Differences in the penetration depths of 660nm and 532nm laser light through varying thicknesses of beef tissue

Light transmission measurement	Red diode laser/ first moments	Red diode laser/within 10 consecutive minutes	Green diode laser/ first moments	Green diode laser/within 10 consecutive minutes
0	31.17±0.30	32.45±0.47	37.33±0.36	36.42±0.19
1	16.33±0.53	13.12±0.64	29.15±0.52	9.41±0.42
3	12.24±0.28	8.31±0.58	4.36±0.17	3.04±0.19
5	10.29±0.18	6.93±0.64	0.90±0.28	0.42±0.22
10	4.47±0.26	3.33±0.08	0.20±0.14	0.11±0.07
20	1.10±0.06	0.90±0.04	0.04±0.0023	0.0003±0.0015
$LSD_{0.05}$	0.507	0.826	0.732	0.331

Table 2. Differences in the penetration depths of 660nm and 532nm laser light through varying thicknesses of chicken breast tissue

Light transmission measurement	Red diode laser/ first moments	Red diode laser/within 10 consecutive minutes	Green diode laser/ first moments	Green diode laser/within 10 consecutive minutes
0	31.57±0.60	32.53±0.23	35.52±0.72	37.08±0.41
1	27.30±0.52	21.6±0.60	20.42±1.10	11.98±0.41
3	9.79±0.17	8.24±0.26	6.44±0.52	4.97±0.38
5	4.69±0.28	2.28±0.51	2.12±0.24	1.27±0.23
10	2.23±0.14	1.14±0.44	1.20±0.13	0.85±0.14
20	1.47±0.23	0.21±0.33	0.12±0.05	0.07±0.03
$LSD_{0.05}$	0.642	0.725	0.574	0.415

Table 3. Multiple comparisons of laser effect between/within groups treated across various thicknesses of beef tissue

	Thickness	N	Mean	Standard deviation	Mean P- value (532 nm)	Mean	Standard deviation	Mean P- value (660 nm)
Irradiated	3	3	104385	13831	0.003	132233	17488	0.001
	5	3	47033	4190	0.001	85611	11943	0.010
	10	3	36222	20669	0.001	54834	16262	0.014
	Total	9	62547	34140	0.003	90893	36293	0.002
Control	3	3	113718	9542	0.124	154966	13397	0.139
	5	3	117983	7330	0.217	147798	4780	0.227
	10	3	136212	9693	0.193	162335	3495	0.080
	Total	9	122638	12913	0.146	155033	9657	0.190

* Means ± SE
*Means with the same difference in the same column are not significantly different

Table 4. Multiple comparisons of laser effect between/within groups treated across various thicknesses of chicken breast tissue

	Thickness	N	Mean	Standard deviation	Mean P- value (532 nm)	Mean	Standard deviation	Mean P- value (660 nm)
Irradiated	3	3	49000	5727	0.001	13821	3094	0.001
	5	3	17166	1595	0.004	24319	4247	0.010
	10	3	24243	6111	0.002	35931	2634	0.006
	Total	9	30136	15090	0.001	24690	10019	0.002
Control	3	3	89330	7388	0.778	38710	2476	0.139
	5	3	91479	4518	0.450	51306	5737	0.227
	10	3	88094	1958	0.450	63267	4934	0.080
	Total	9	89634	4680	0.626	51095	11355	0.136

* Means ± SE
*Means with the same difference in the same column are not significantly different.

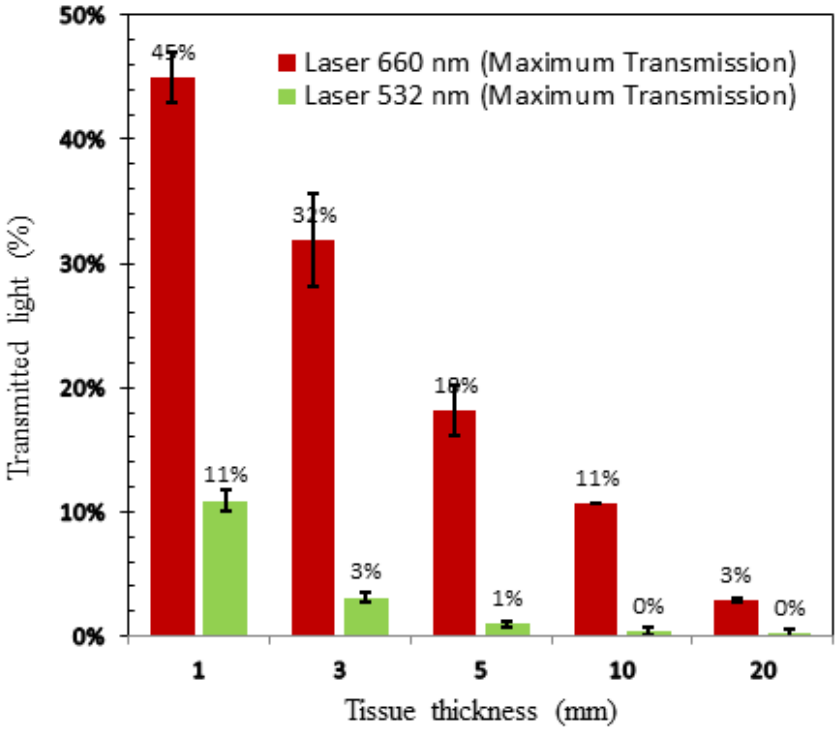

Figure 4. The maximum transmittance of laser light at 660 nm and 532 nm across various thicknesses of beef tissue for more than 10 consecutive minutes

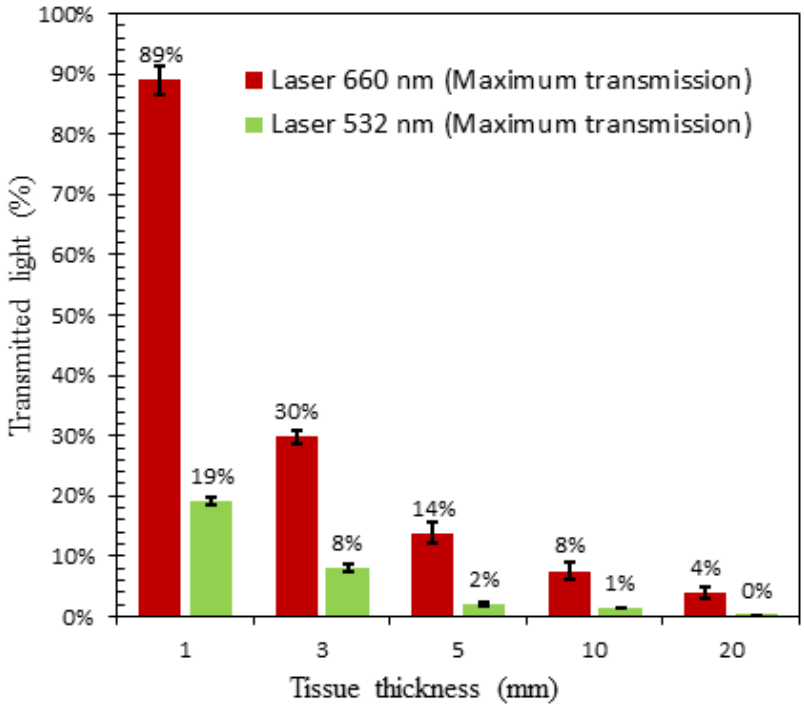

Figure 5. The maximum transmittance of laser light at 660 nm and 532 nm across various thicknesses of chicken breast tissue for more than 10 consecutive minutes.

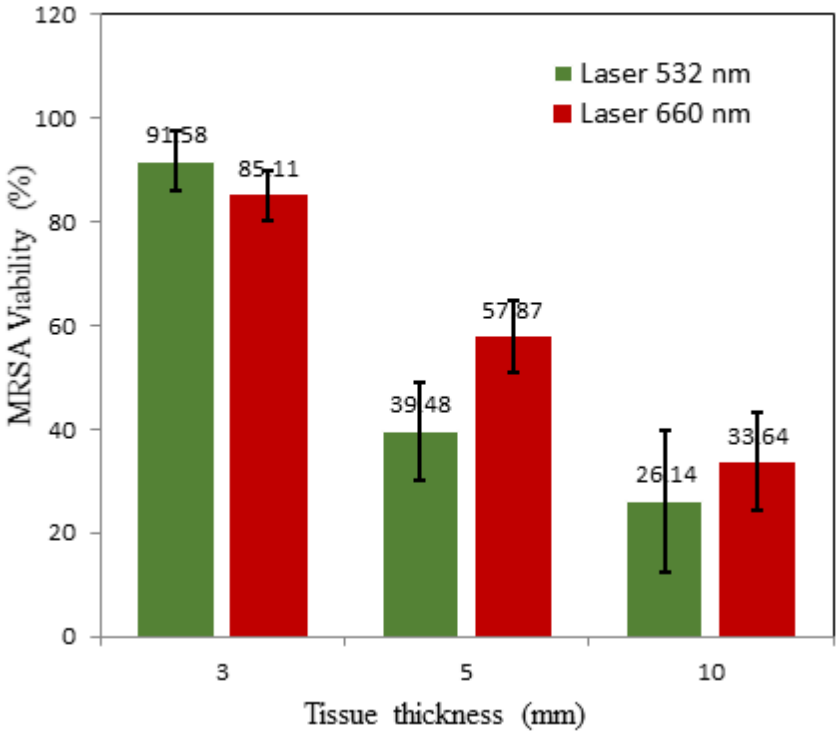

Figure 6. The percentage of MRSA viability after irradiation with wavelengths of 660 nm and 532 nm for various beef tissue thicknesses

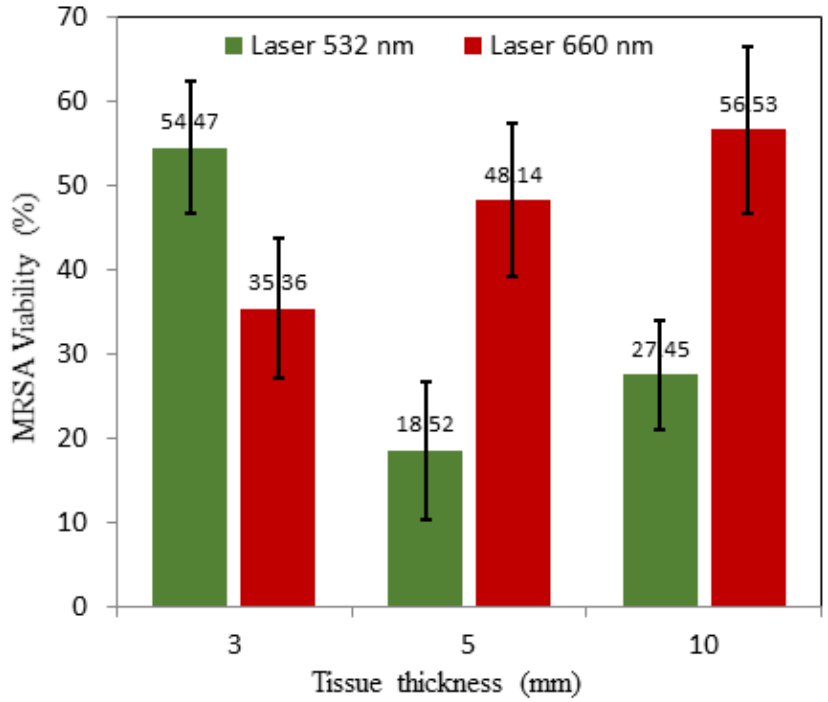

Figure 7. The percentage of MRSA viability after irradiation with wavelengths of 660 nm and 532 nm for various chicken tissue thicknesses.

5. Conclusions

In conclusion, a comparative analysis of the effects of 532 nm and 660 nm diode lasers on MRSA contamination in different tissue thicknesses provides valuable insights into the complex dynamics of laser-based microbial control. The wavelength-specific effects, coupled with tissue thickness considerations and specific interaction effects emphasize the need for precision in the design of laser interventions. Moreover, considerations of penetration depth and transmission properties are essential to optimize laser-based microbial control strategies, ensuring precise targeting of pathogens while minimizing collateral tissue damage. These findings contribute to advance the understanding of optimal strategies for microbial decontamination, emphasizing the importance of a multifaceted approach in clinical practice.

Funding: This research was supported by the Ministry of Higher Education Malaysia under the Fundamental Research Grant Scheme with Project Code: FRGS/1/2021/STG0 7/USM/02/5.

Acknowledgments: This research was supported by the Ministry of Higher Education Malaysia under the Fundamental Research Grant Scheme with Project Code: FRGS/1/2021ST G07/USM/02/5. The authors would like to thank the School of Physics, Universiti Sains Malaysia, and Al-Qadisiyah University, College of Veterinary Medicine, Iraq for their support in the present work.

Conflict of Interest: The authors declared no potential conflicts of interest.

Data Availability Statement: The corresponding author can provide the data described in this study upon request

References

[1] V. H. Matsubara, B. W. Leong, M. J. L. Leong, Z. Lawrence, T. Becker, and A. Quaranta, "Cleaning potential of different air abrasive powders and their impact on implant surface roughness," Clin. Implant Dent. Relat. Res., vol. 22, no. 1, pp. 96–104, 2020.

[2] K. Wang, H. Pu, and D. Sun, "Emerging spectroscopic and spectral imaging techniques for the rapid detection of microorganisms: An overview," Compr. Rev. food Sci. food Saf., vol. 17, no. 2, pp. 256–273, 2018.

[3] P. Nandhini, P. Kumar, S. Mickymaray, A. S. Alothaim, J. Somasundaram, and M. Rajan, "Recent developments in methicillin-resistant Staphylococcus aureus (MRSA) treatment: A review," Antibiotics, vol. 11, no. 5, p. 606, 2022.

[4] M. Qi et al., "Novel nanomaterial-based antibacterial photodynamic therapies to combat oral bacterial biofilms and infectious diseases," Int. J. Nanomedicine, pp. 6937–6956, 2019.

[5] S. Bordin-Aykroyd, R. B. Dias, and E. Lynch, "Laser-tissue interaction," EC Dent Sci, vol. 18, pp. 2303–2308, 2019.

[6] J. Zhou et al., "Impact of lanthanide nanomaterials on photonic devices and smart applications," Small, vol. 14, no. 40, p. 1801882, 2018.

[7] M. R. Hamblin, T. Agrawal, and M. de Sousa, Handbook of low-level laser therapy. CRC Press, 2016.

[8] G. Keiser and G. Keiser, "Light-tissue interactions," Biophotonics Concepts to Appl., pp. 147–196, 2016.

[9] R. A. Mussttaf, D. F. L. Jenkins, and A. N. Jha, "Assessing the impact of low level laser therapy (LLLT) on biological systems: a review," Int. J. Radiat. Biol., vol. 95, no. 2, pp. 120–143, 2019.

[10] R. Cave, J. Cole, and H. V Mkrtchyan, "Surveillance and prevalence of antimicrobial resistant bacteria from public settings within urban built environments: Challenges and opportunities for hygiene and infection control," Environ. Int., vol. 157, p. 106836, 2021.

[11] N. P. Vitko and A. R. Richardson, "Laboratory maintenance of methicillin-resistant Staphylococcus aureus (MRSA)," Curr. Protoc. Microbiol., vol. 28, no. 1, pp. 9C–2, 2013.

[12] C. D. Cruz, S. Shah, and P. Tammela, "Defining conditions for biofilm inhibition and eradication assays for Gram-positive clinical reference strains," BMC Microbiol., vol. 18, no. 1, pp. 1–9, 2018.

[13] Z. A. Aiken, "Measuring the susceptibility and adhesion of microorganisms to light-activated antimicrobial surfaces." UCL (University College London), 2012.

[14] A. Cios et al., "Effect of different wavelengths of laser irradiation on the skin cells," Int. J. Mol. Sci., vol. 22, no. 5, p. 2437, 2021.

[15] E. Ahmed, A. O. El-Gendy, M. R. Hamblin, and T. Mohamed, "The effect of femtosecond laser irradiation on the growth kinetics of Staphylococcus aureus: An in vitro study," J.

Photochem. Photobiol. B Biol., vol. 221, p. 112240, 2021.
[16] E. Khalkhal, M. Razzaghi, M. Rostami-Nejad, M. Rezaei-Tavirani, H. H. Beigvand, and M. R. Tavirani, "Evaluation of laser effects on the human body after laser therapy," J. Lasers Med. Sci., vol. 11, no. 1, p. 91, 2020.
[17] A. A. Aldalawi et al., "Comparison of Wavelength-Dependent Penetration Depth of 532 nm and 660 nm Lasers in Different Tissue Types," J. Lasers Med. Sci., vol. 14, 2023.
[18] H. Liu, Y. Zhang, Y. Hu, and Z. Tse, "Laser Power Transmission and Its Application in Laser-Powered Electrical Motor Drive: A Review," Power Electron. Drives, vol. 6, no. 1, pp. 167–184, 2021.
[19] Y. Zhang et al., "pH-responsive hierarchical H2S-releasing nano-disinfectant with deep-penetrating and anti-inflammatory properties for synergistically enhanced eradication of bacterial biofilms and wound infection," J. Nanobiotechnology, vol. 20, no. 1, p. 55, 2022.
[20] A. Zapata and S. Ramirez-Arcos, "A comparative study of McFarland turbidity standards and the Densimat photometer to determine bacterial cell density," Curr. Microbiol., vol. 70, pp. 907–909, 2015.
[21] M. A. Islam, M. M. Alam, M. E. Choudhury, N. Kobayashi, and M. U. Ahmed, "Determination of minimum inhibitory concentration (MIC) of cloxacillin for selected isolates of methicillin-resistant Staphylococcus aureus (MRSA) with their antibiogram.," 2008.
[22] L. Shao, S. Majumder, Z. Liu, K. Xu, R. Dai, and S. George, "Light activation of gold nanorods but not gold nanospheres enhance antibacterial effect through photodynamic and photothermal mechanisms," J. Photochem. Photobiol. B Biol., vol. 231, p. 112450, 2022.
[23] H. E. ElZorkany, T. Youssef, M. B. Mohamed, and R. M. Amin, "Photothermal versus photodynamic treatment for the inactivation of the bacteria Escherichia coli and Bacillus cereus: an in vitro study," Photodiagnosis Photodyn. Ther., vol. 27, pp. 317–326, 2019.
[24] M. A. Triana, A. A. Restrepo, R. J. Lanzafame, P. Palomaki, and Y. Dong, "Quantum dot light-emitting diodes as light sources in photomedicine: photodynamic therapy and photobiomodulation," J. Phys. Mater., vol. 3, no. 3, p. 32002, 2020.
[25] S. Mallidi, S. Anbil, A.-L. Bulin, G. Obaid, M. Ichikawa, and T. Hasan, "Beyond the barriers of light penetration: strategies, perspectives and possibilities for photodynamic therapy," Theranostics, vol. 6, no. 13, p. 2458, 2016.
[26] V. V Tuchin, "Tissue optics and photonics: light-tissue interaction," J. Biomed. Photonics Eng., vol. 1, no. 2, pp. 98–134, 2015.
[27] S. Kumari and A. K. Nirala, "Study of light propagation in human and animal tissues by Monte Carlo simulation," Indian J. Phys., vol. 86, pp. 97–100, 2012.
[28] F. H. Mustafa and M. S. Jaafar, "Comparison of wavelength-dependent penetration depths of lasers in different types of skin in photodynamic therapy," Indian J. Phys., vol. 87, no. 3, pp. 203–209, 2013.
[29] J. Hong, W. Guan, G. Jin, H. Zhao, X. Jiang, and J. Dai, "Mechanism of tachyplesin I injury to bacterial membranes and intracellular enzymes, determined by laser confocal scanning microscopy and flow cytometry," Microbiol. Res., vol. 170, pp. 69–77, 2015.
[30] A. A. K. Al-Shammary, N. A. A. Mohd Ma'amor, S. Q. Chen, K. S. Lee, and K. Mohd Hanafiah, "Bactericidal effects of in vitro 405 nm, 530 nm and 650 nm laser irradiation on methicillin-resistant Staphylococcus aureus, Pseudomonas aeruginosa and Mycobacterium fortuitum," Lasers Dent. Sci., vol. 4, no. 3, pp. 111–121, 2020.